

# Adsorption of Indium on a InAs wetting layer deposited on the GaAs(001) surface

Marcello Rosini\* and Rita Magri

*Dipartimento di Fisica dell'università degli studi di Modena  
e Reggio Emilia and S3 research center of CNR-INFM,  
via Campi 213/A, 41100 Modena, Italy*

Peter Kratzer

*Fachbereich Physik, Universität Duisburg-Essen, Germany*

(Dated: October 31, 2018)

## Abstract

In this work we perform a first-principles study of the adsorption properties of an In adatom deposited on 1.75 monolayers (ML) InAs, forming a wetting layer on GaAs(001) with the  $\alpha_2(2 \times 4)$  or  $\beta_2(2 \times 4)$  reconstruction. The structural properties of these reconstructions have been studied: we determine the equilibrium geometry of the surfaces and their stability for various growth conditions. We have then carried out a detailed study of the potential energy surface (PES) for an In adsorbate, finding the minima and the saddle points. The main characteristics of the PES and the bonding configurations of the In adatom on the surface are analyzed by comparing with analogous studies reported in the literature, trying to extract the effects due to: (i) the compressive strain to which the InAs adlayer is subjected, (ii) the particular surface reconstruction, and (iii) the wetting layer composition. We found that, in general, stable adsorption sites are located at: (i) locations besides the As in-dimers, (ii) positions bridging two As in-dimers, (iii) between two adjacent ad-dimers (only in  $\beta_2$ ), and (iv) locations bridging two As ad-dimers. We find also other shallower adsorption sites which are more reconstruction specific due to the lower symmetry of the  $\alpha_2$  reconstruction compared to the  $\beta_2$  reconstruction.

PACS numbers: 68.43.Jk, 31.50.-x

---

\*Electronic address: mrosini@unimo.it

## I. INTRODUCTION

Thanks to the strong charge carrier confinement, QDs have atomic-like properties that could be useful for applications in optical and optoelectronic devices, quantum computing, and information storage. One of the most challenging problems for quantum dot formation, is the control of their shape, composition and density. From this point of view the abundant experimental knowledge has not yet produced a sufficiently deep understanding of the physics of formation of quantum dots that could guide the way to control the growth process. In this situation first-principles simulations can be helpful in shedding light on the atomistic mechanisms that lead to dot nucleation at surfaces.

In the present paper, we address one of the most-studied systems: InAs quantum dots grown on a GaAs(001) substrate, where the lattice mismatch between InAs and GaAs is of the order of 7%. Strain relaxation at the surface acts as a driving force for a self-assembly process, the so called Stranski-Krastanov growth mode [1], with the deposition of an atomically thin InGaAs wetting layer (WL) and subsequent surface mass transport accompanied by a 2D to 3D growth transition.

We focus our attention on the structural properties of the WL on which quantum dots nucleate, and on the interaction between a single In adatom and the surface, in order to find where the diffusion barriers are located and what the possible adsorption sites on the surface are, as a function of the wetting layer reconstruction.

We have chosen to investigate mainly the  $\alpha_2(2 \times 4)$  reconstruction of the (001) surface because of its stability under In-rich conditions and under compressive strain [2, 3, 4] which is the case for the InAs WL grown on GaAs. Moreover, a  $(2 \times 4)$  reconstruction was found [5, 6, 7, 8] to occur on the (001) wetting layer at the onset of dot nucleation in a In-rich WL condition. We have modeled a WL at a InAs coverage  $\theta = 1.75$  monolayer (ML) which is close to the critical value corresponding to the 2D to 3D transition [9]. The structural and geometrical properties of this surface have been investigated. Using the  $\alpha_2$  reconstruction we have calculated the PES for a single In adatom, with the aim to understand what are the implications of the WL morphology (strain and composition) on the adsorption and surface mobility of the deposited In. To this end a comprehensive comparison with results reported previously in the literature for Ga and In adatoms and other surface reconstructions is given. In this context, a detailed analysis of the differences and analogies between the  $\alpha_2$  and the

$\beta_2$  reconstructions is pursued.

In the literature similar calculations have been reported for GaAs [100] homoepitaxy [10]. The issue of the WL composition for In adsorption has been addressed only by Penev et. al. [11, 12], but for a much lower In coverage of  $\theta = 0.66$  ML.

The paper is organized as follows: in section II we detail our theoretical approach. Section III reports the obtained results for: (i) the WL surface reconstruction and energy; (ii) the PES of a single In adatom on the  $\alpha_2$  and the  $\beta_2$  reconstructed WL; (iii) the determination of the barrier positions and heights between each couple of adsorption sites; (iv) a detailed study of the atomic bonding of the In adatom to the WL. In section IV our results are compared with those regarding other surface reconstructions in order to extract a rationale for the dependence on In adsorption and diffusion on the local structure of the (001) surface. Finally, a summary is given at the end of the paper.

## II. THEORETICAL METHOD

We performed first principles calculations within Density Functional Theory in the local density approximation (DFT-LDA) [13] using the exchange and correlation potential of Ceperley and Alder [14] as parametrized by Perdew and Zunger [15]. For this kind of calculations both LDA [2, 16, 17, 18, 19] and GGA [10, 12, 20, 21, 22] have been used in the literature. It has been demonstrated [23, 24] that both methods give qualitatively the same picture for the description of adatom adsorption on a surface, although LDA usually gives larger values for binding energies than GGA [25]. Only the details can be different: LDA tends to overestimate the binding energy but for lattice constants, elastic moduli and surface energies the LDA calculated values are generally closer to the experimentally determined ones. We have used norm-conserving pseudopotentials treating the outermost s- and p-shells of Ga, In and As as valence electrons, and the electronic wave functions were expanded in plane-waves, with a 18 Ry kinetic energy cutoff. The energy cutoff has been tested in order to reach convergence for the lattice bulk properties of GaAs and InAs. The core corrected atomic pseudopotentials have been tested on bulk Ga, In and As, where the determined equilibrium configurations and elastic moduli compare well with the experimental data.

The equilibrium lattice parameters obtained for the GaAs and InAs bulk phases are  $a_0 = 5.609$  Å and  $a_0 = 5.906$  Å, which are slightly smaller than the experimental ones.

Thus our calculated lattice mismatch is 5.4%, smaller than the experimental value. This is going to underestimate the WL strain. In sec. IV we will compare our results with results [10, 12, 16] where this effect was instead overestimated.

Starting from the GaAs structure, we have set up the (001) oriented supercell containing 4 layers of GaAs, covered with 1.75 layers of InAs arranged according to the  $\alpha_2(2 \times 4)$  surface reconstruction. The lower layer of Ga atoms is kept fixed during the cell relaxation, in order to mimic the constraint due to the underlying semi-infinite bulk, and it is passivated with pseudo hydrogen atoms of 1.25 electron charge. The slab is repeated along the (001) direction with a periodicity  $5a_0$  and a separation of about 10 Å of vacuum. As for the number of GaAs layers, we have found that only two layers suffice to obtain a correct description of the PES, minima and maxima positions. The refinement using two more GaAs layers produces a difference in the barrier heights all within 40 meV. Brillouin-zone (BZ) integration was carried out using a set of special  $k$ -points equivalent to 16 points in the  $1 \times 1$  surface BZ. A smearing of 0.02 Ry has been used in order to account for the possible metalization of the surface electronic structure.

In the  $\alpha_2(2 \times 4)$  reconstruction the last complete atomic layer is constituted by As atoms. A  $\theta = 0.75$  cation layer is deposited over it. This layer is then terminated with one As dimer (As ad-dimer) on top (see Fig. 1). The uncovered As on the last complete layer dimerizes along the  $[\bar{1}10]$  direction (As in-dimer). The  $\beta_2(2 \times 4)$  reconstruction is similar but presents one additional As ad-dimer bridging the two remaining In rows on the top of the surface (see Fig. 1). It has a larger symmetry than the  $\alpha_2$  reconstruction, being mirror symmetric with respect to the (110) plane passing through the As in-dimers. All the examined structures have been relaxed in order to find the equilibrium geometries, until all the forces acting on the atoms were less than  $2.5 \cdot 10^{-3}$  eV/Å.

The PES of an In adatom is calculated by relaxing the adatom  $z$  component together with all the surface degrees of freedom while the in-plane  $x$ ,  $y$  coordinates are kept fixed. We have set up a grid of  $8 \times 4$  points, corresponding to a step of 2 Å, along the (110) and  $(\bar{1}10)$  directions respectively, and for each point we have found the minimum energy configuration for the adsorbate plus surface. Then we have interpolated the grid data with a bi-cubic spline algorithm in order to find the positions of the minima and the saddle points. The exact values of the minima have then been determined by further relaxing all the three coordinates of the adatom together with the surface. To minimize the adsorbate interaction

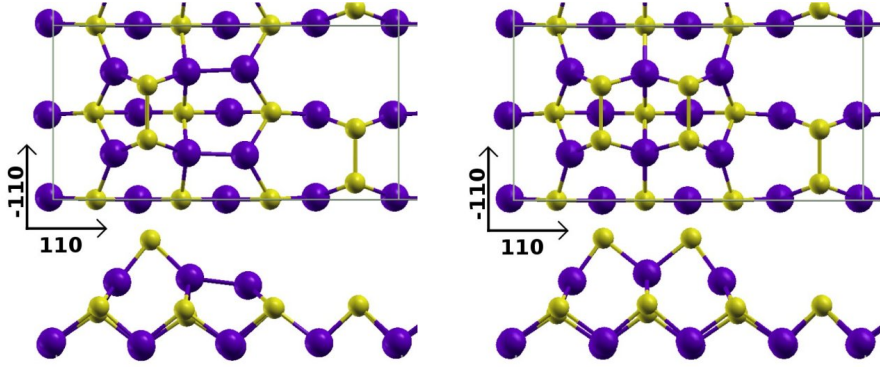


FIG. 1: (Color online) Representation of the  $\alpha_2(2 \times 4)$  (left) and  $\beta_2(2 \times 4)$  (right) surface reconstructions. The shown geometries are those optimized. It is evident the bending of the the In-In bond in the top layer in the  $\alpha_2$  reconstruction. Dark balls and light balls represent In and As ions respectively.

we have doubled the surface unit cell along the  $(\bar{1}10)$  direction.

Since one of the objectives of this work is ultimately to study In diffusion on the WL within the framework of the Transition State Theory [26, 27, 28], the minimum energy paths (MEP) and the height of each energy barrier between every couple of adsorption sites have to be calculated, leading to a more detailed knowledge of the PES. This task has been accomplished by using the Nudged Elastic Band method (NEB). This method is able to find the MEP between two adsorption sites, by simulating a string of replicas of the system, where the different images are one linked to the other by springs [29, 30]. By minimizing the energy associated to the path, an accurate description of the MEP and thus of the saddle point is obtained.

All the ab-initio calculations were performed using the ESPRESSO simulation package [31].

### III. RESULTS

#### A. Structure of $(001)(2 \times 4)$ surface reconstructions

We have calculated the optimized geometries and the formation energies of the  $\alpha_2(2 \times 4)$  and  $\beta_2(2 \times 4)$  reconstructions of the bare GaAs surface and of GaAs covered with a  $\theta = 1.75$  ML InAs layer. The surface energies vs. the As chemical potential  $\mu_{As}$  (whose value is

related to the growth conditions such as growth temperature, cation/anion flux ratios) are calculated through the expression [32]

$$\gamma_f = \frac{1}{A} (E_{\text{tot}} - N_{\text{Ga}}\mu_{\text{GaAs}} - N_{\text{In}}\mu_{\text{InAs}}) - \mu_{\text{As}} \frac{N_{\text{As}} - N_{\text{Ga}} - N_{\text{In}}}{A}, \quad (1)$$

( $\mu_{\text{InAs}} = 0$ ,  $N_{\text{In}} = 0$  for pure GaAs). The obtained surface energies are reported in Fig. 2. Here  $E_{\text{tot}}$  is the total energy of the slab,  $\mu_{\text{xx}}$  is the chemical potential of the bulk phase of material xx,  $N_y$  is the number of atoms of element y in the supercell and  $A$  is the surface unit cell area. A set of calculations is performed for a slab with two hydrogen passivated surfaces, in order to subtract the contribution of the bottom surfaces of the reconstructed slabs to be investigated, hence  $E_{\text{tot}}$  is the net contribution of the reconstructed slab. Elemental As, Ga and In are calculated using their ground state structures: respectively the rhombohedral A7 structure for As,  $\alpha$ -Ga and bct In. All these calculations have been done using high convergence standards. We see that the range of stability of the  $\alpha_2$  phase, when GaAs is covered with the InAs ad-layer, is larger than that of the bare GaAs surface. This means that the formation of the  $\alpha_2$  phase will be favored over the  $\beta_2$  phase over a larger range of As flux values (or surface growth conditions), when the InAs WL is formed. This is in agreement with previous calculations showing a stabilization of the  $\alpha_2$  phase for InAs under isotropic compressive strain [2, 11] which is the condition of the InAs layer grown on GaAs.

Regarding the atomic structures, the comparison of the distances between the atomic planes, in the InAs covered GaAs case, shows that the values are systematically larger than those obtained for the pure GaAs surface by about 10 %, owing to the stress originated by the InAs/GaAs lattice mismatch. In particular, we remark the buckling of the bond between the In atoms in the uncompleted In layer found for the  $\alpha_2$  reconstruction (see Fig. 1) due to the missing (with respect to the  $\beta_2$  reconstruction) second As ad-dimer. It was shown ([2]) that this buckling plays a role in the stabilization of the  $\alpha_2$  phase.

## B. The potential energy surface of the single In adatom

In the following we describe our calculations for both the  $\alpha_2$  and  $\beta_2$  surface reconstructions, with an accurate description of the adsorption sites and hopping barriers.

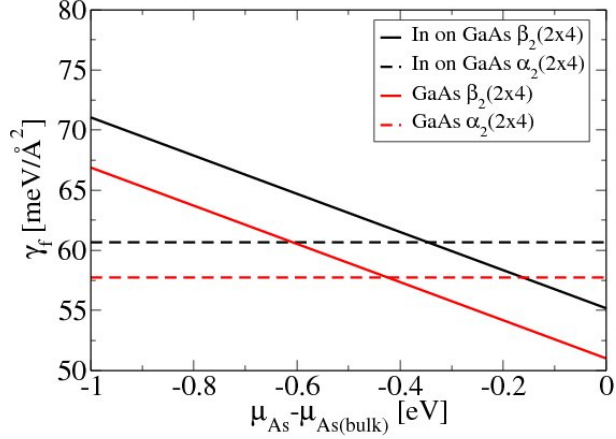


FIG. 2: (Color online) Surface energy phase diagram for the  $\alpha_2(2 \times 4)$  and  $\beta_2(2 \times 4)$  reconstructions of InAs/GaAs(001) and GaAs(001).

### 1. $\alpha_2(2 \times 4)$ surface reconstruction

For this surface reconstruction we have found eleven adsorption sites for the In adatom, and the related saddle points. The energies of the minima and of the saddle points are given in Tables I and II, respectively, and a graphical representation of the PES is reported in Fig. 3. In the Tables, the energies are relative to that of the deepest adsorption site  $A_8$  put to 0. Two main low potential trenches are evident along the  $[\bar{1}10]$  direction, at both sides of the As in-dimer row. The deepest adsorption site  $A_8$  is located in the trench near the In vacancy of the surface layer and is bonded to the two As atoms of the in-dimer and to one In atom (see Fig. 4(a)). Other deep minima ( $A_4$ ,  $A_6$ , and  $A_9$ ) are located along the two deepest trenches and, together with  $A_8$ , represent the lowest energy set of minima. Their adsorption configuration is similar to that of  $A_8$ . A second class of adsorption sites ( $A_1$ ,  $A_3$ ,  $A_5$ ,  $A_{11}$ ) is characterized by the In adatom bonded to two other In atoms (see the configuration at minimum  $A_5$  in Fig. 4(b)). At the minima  $A_7$  and  $A_2$  the adatom is bonded to four In atoms, reproducing the bonding scheme typical of bulk Indium (Fig. 4(c)). In these last cases the corresponding surface electronic structure is metallic. To the last class of adsorption sites belongs the shallow minimum  $A_{10}$  where the adatom is bonded to the two As of the ad-dimer (see Fig. 4(d)). This configuration plays the role of a precursor for the much stronger bonding of In into the ad-dimer (see below).

We have accurately checked that the shallow minima in the PES are actually minima and

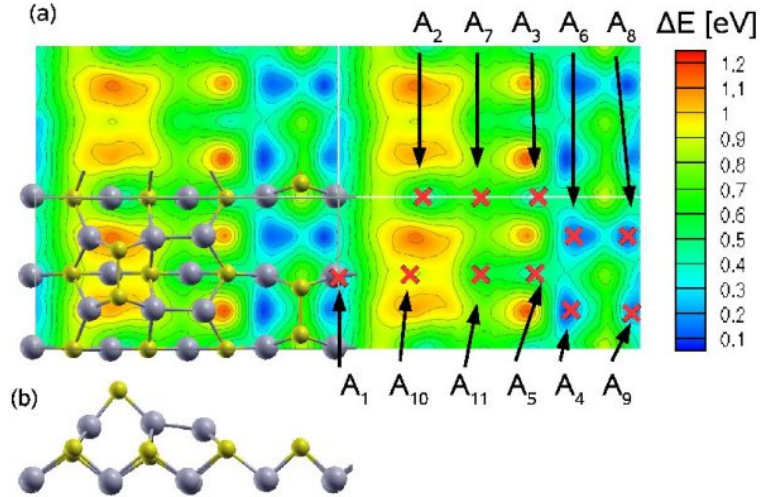


FIG. 3: (Color online) (a) PES of an In adatom on the  $\alpha_2$  ( $2 \times 4$ ) surface. The PES is drawn for 4 surface unit cells and a top view of the atomic structure is also shown. The minima are labeled  $A_i$ . (b) Side view of the surface layer.

not saddle points of the energy landscape.

The location of the calculated barriers  $T_n$  is shown in Fig. 5(a). The barriers are lower along the  $[\bar{1}10]$  direction (the highest barrier being 430 meV and the lowest being 52 meV) than along the orthogonal  $[110]$  direction (see Table II). This difference is mainly ascribed to the presence of the As ad-dimer oriented along the  $[\bar{1}10]$  direction, that creates an unstable region for the In adsorption, as can be seen in the PES of Fig 3. From these considerations we can preliminarily conclude that adatom surface diffusion should be strongly anisotropic with the  $[\bar{1}10]$  direction along the trenches favored.

## 2. $\beta_2(2 \times 4)$ surface reconstruction

Since the symmetric part of the  $\beta_2$  has the same structure of half of the  $\alpha_2$  surface, the coordinates of the adsorption sites can be roughly estimated, and their exact location can be found with a further relaxation of the surface-adsorbate system.

Also for the  $\beta_2$  surface reconstruction, we have found 11 adsorption sites for the Indium adatom (see Table III and Fig. 5(b)). However, owing to the symmetry properties of the system, those minima reduce to only 6 inequivalent minima.

We first notice that the adsorption sites  $A_1, A_2, A_4, A_6, A_7, A_8, A_9$ , are in strict corre-

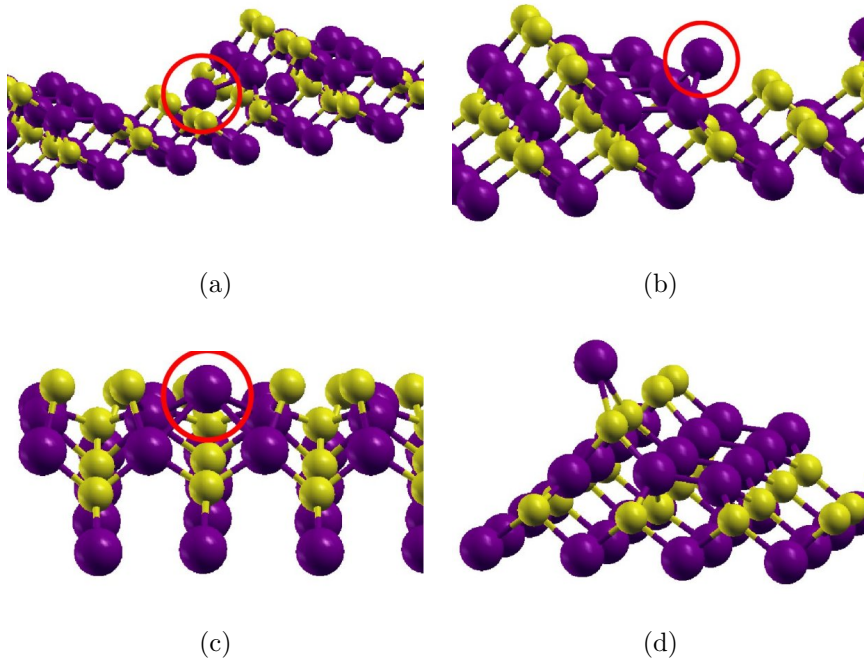


FIG. 4: (Color online) Adsorption configurations for the In adatom in different adsorption sites on the  $\alpha_2$  surface reconstruction. (a) Configuration  $A_8$  (b) Configuration  $A_5$  (c) Configuration  $A_2$  (d) Configuration  $A_{10}$

spondence to those of the  $\alpha_2$  surface reconstruction (see Fig 5), in the region where the two structures are similar i.e. far from the  $\beta_2$  second ad-dimer. The positions of the minima are only slightly affected by the presence of the extra As ad-dimer, and the deepest adsorption site  $A_8$  lies in the same position as for the  $\alpha_2$  reconstruction. The minima  $A_3$  and  $A_5$  are shifted towards the trench with respect to the corresponding ones of the  $\alpha_2$  reconstruction. This is due to the fact that the In adatoms in  $A_3$  and  $A_5$  on the  $\alpha_2$  reconstruction are bonded to the buckled In at the trench edge. The same In is not buckled in  $\beta_2$  due to its bond to the second As ad-dimer row (compare Fig. 4(b) to Fig. 6(a)). To quantify the difference between the  $A_1$ - $A_9$  adsorption sites in the two reconstructions, we give in Table IV the adsorption energy difference  $\Delta E = E^\beta(A_i) - E^\alpha(A_i)$  (negative if In is more strongly bonded in the  $\beta_2$  than in  $\alpha_2$  reconstruction) and the displacement  $\Delta r = \sqrt{\sum_i (r_i^\beta - r_i^\alpha)^2}$  between the corresponding binding locations. The adsorption energy is defined as

$$E^\alpha(A_i) = E(\alpha_2 + \text{In}_{A_i}) - E(\alpha_2) - E(\text{In}) . \quad (2)$$

In  $\beta_2$ ,  $A_3'$  Fig 5 is the symmetric of the minimum  $A_3$ . This minimum is not present in the

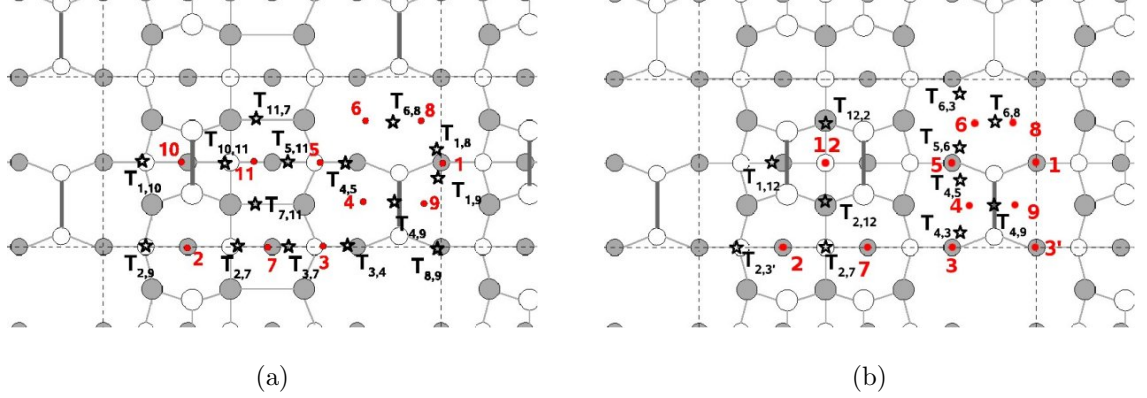


FIG. 5: (Color online) Schematic view of the adsorption sites locations (only  $i$  is written) on the: (a)  $\alpha_2$  ( $2 \times 4$ ) and (b)  $\beta_2$  ( $2 \times 4$ ) reconstructions. The saddle points are labeled as  $T_{i,j}$ .

$\alpha_2$  reconstruction because of the lower symmetry. A new minimum  $A_{12}$  is now present for  $\beta_2$  on top of the two ad-dimers and it is actually quite stable, since the In-atom is fourfold bonded to the surface (see fig. 6(b)). In this case the confinement barriers are calculated to be of the order of 135 meV. The configuration for In in the adsorption sites different from those of the  $\alpha_2$  reconstruction, are given in Fig. 6.

Also in the  $\beta_2$  case, two trenches in the PES are evident along the  $(\bar{1}10)$  direction at both sides of the As in-dimer. The existence of the  $A_{12}$  adsorption site on  $\beta_2$  could originate additional diffusion paths along the same direction connecting the minimum  $A_{12}$  to the two sites  $A_2$  and  $A_7$ . The corresponding saddle point energies are reported in Table V. We can easily see that the barriers along  $[\bar{1}10]$ , are in the range 100-580 meV and are lower than the barriers along the  $[110]$  direction that span the range 100-760 meV. This consideration strongly indicates that also for the  $\beta_2$  surface reconstruction, the In-atom diffusion should be highly favored along the  $(\bar{1}10)$  direction.

### C. Additional adsorption sites due to In insertion in the As dimers

We know from the literature [16, 20] that additional minima could be present, corresponding to the In atom breaking the bond between the As adatoms in a dimer and binding itself to them. This process requires overcoming an energy barrier, thus its rate should depend on the growth temperature. These sites can be of significant interest, since they introduce a local modification of the PES that can be very important for surface diffusion.

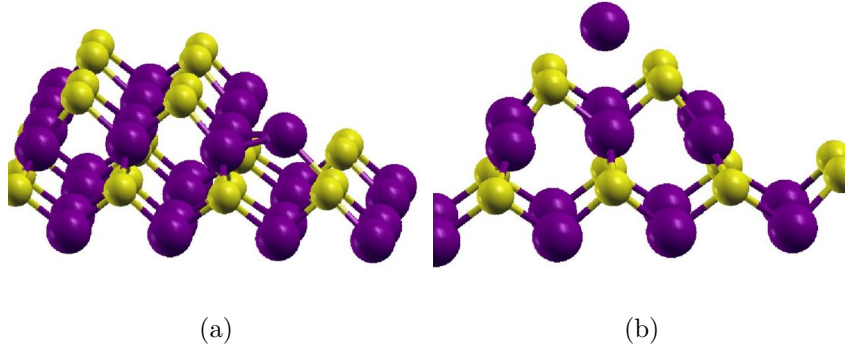


FIG. 6: (Color online) Adsorptions configurations for the In adatom on the  $\beta_2$  surface reconstruction. (a) Configuration  $A_5$  (b) Configuration  $A_{11}$

For example, such sites could be in a bridge location between two other adsorption sites, thus introducing a further minimum in an otherwise thicker barrier. Such an additional adsorption site can affect the diffusion kinetics of the In adatom on the surface.

We have considered both the As in-dimers and ad-dimers of the  $\alpha_2$  and  $\beta_2$  surface reconstructions and determined the energy necessary to break the As-As bond and bind the In adatom. First of all we have put In in the middle between the two As atoms, in a vertical plane containing all the three atoms. We have then relaxed the system obtaining the minimum energy position for the In adatom. Finally we have performed different NEB calculations in order to find the energy barriers between these adsorption sites and the neighboring sites. We have found that the adsorption configuration with the In atom bonded to the two arsenic of the dimers are in general more stable than most of the other adsorption sites (see Tables I and III).

### 1. $\alpha_2(2 \times 4)$ surface reconstruction

In this case we have found 2 additional stable sites for the In adsorbate. The first one corresponds to the breaking of the As ad-dimer and the second one to the breaking of the As in-dimer. The two cases are shown in figures 7 and 8, respectively. Figures 7(a) and 8(a) show the location of these minima, indicated as  $A_a$  and  $A_i$  respectively, on the surface ( $a$  =ad-dimer  $i$  =in-dimer). Figures 7(b) and 8(b) show the atomic configuration of the adsorbate bonded to the As atoms in the dimers. The transitions to/from neighboring adsorption sites are also drawn in the figures (Figs. 7(c) and 8(c)) and the corresponding

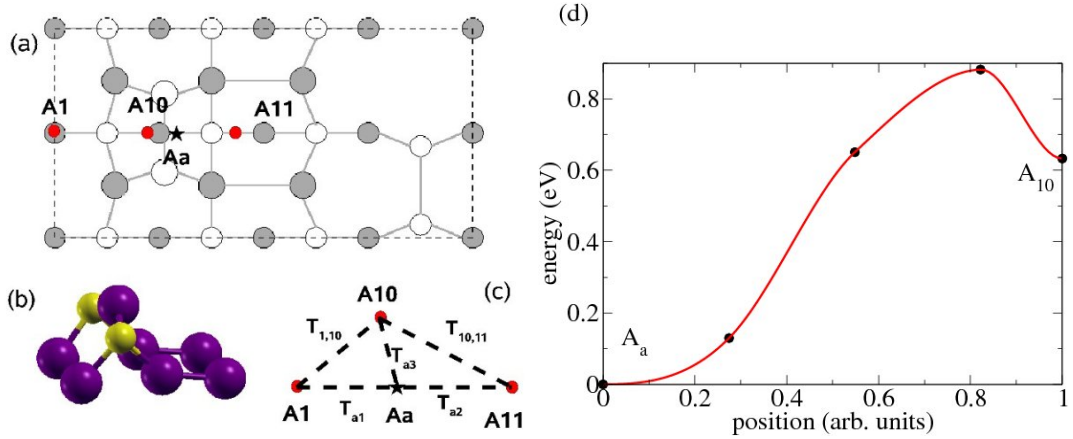


FIG. 7: (Color online) Additional adsorption site  $A_a$  due to the In insertion into the As ad-dimer on the  $\alpha_2$  reconstruction. (a) The location of the adsorption site is indicated by a star. (b) Atomic configuration. (c) Scheme of the transitions between the  $A_a$  adsorption site and the neighboring sites. (d) Energy profile for barrier  $T_{a3}$  from the precursor site  $A_{10}$  to  $A_a$ .

minima and saddle point energies are given in Tables I and II respectively. We can see that those minima are deep and stable, since the confining barriers ( $\simeq 0.8$  eV), pictured in Figures 7(d) and 8(d) are high. The energy barrier needed to fall into  $A_a$  from the site  $A_{10}$  (the precursor site) is not too high (around 200 meV) and this process is likely to occur even at relatively low temperature.

## 2. $\beta_2(2 \times 4)$ surface reconstruction

In this case we have two As ad-dimers instead of one. We have found one adsorption site for the In adatom for each one of the ad-dimers indicated in Figures 9 as  $A_{a1}$  and  $A_{a2}$ . We have found that the In adsorbate does not lie in the vertical plane passing through the As dimers, but the bonds are tilted towards the other ad-dimer, that is towards the symmetry plane passing through the  $A_{12}$  adsorption site. Regarding the As in-dimer we have found two distinct possibilities for In adsorption that we indicate as  $A_{i1}$  and  $A_{i2}$  in Figure 10. As can be seen from Fig. 10(b), the In atom bonds to the two As of the in-dimer forming a tilted angle  $\phi$  with respect to the vertical  $z$  direction. Since the (110) is a plane of symmetry for the system, the two configurations for the adsorbate, corresponding to angles  $\phi$  and  $-\phi$ , with respect to the  $z$  axis are equivalent and have the same probability to occur.

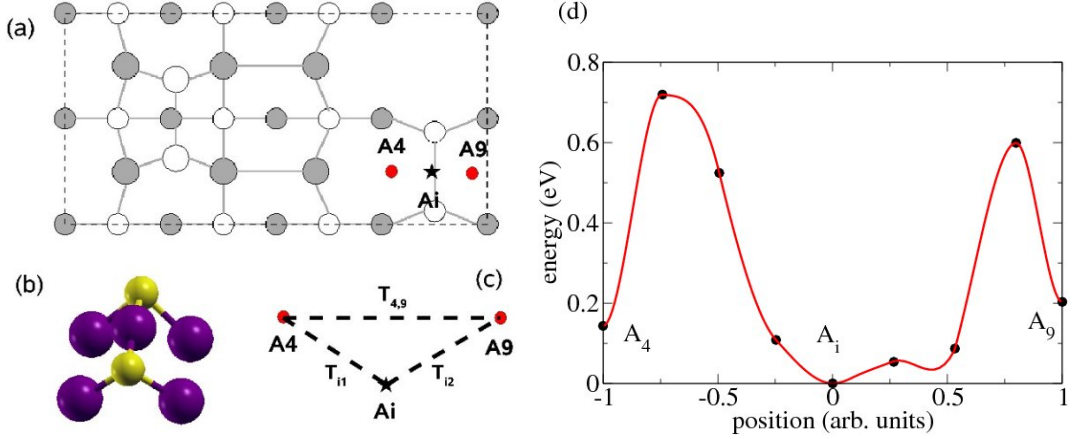


FIG. 8: (Color online) Additional adsorption site  $A_i$  due to the In insertion into the As in-dimer on the  $\alpha_2$  surface reconstruction. (a) The location of the adsorption site is indicated by a star. (c) Atomic configuration. (b) Scheme of the transitions between the  $A_i$  adsorption site and the neighboring sites. (d) Energy profile for barriers  $T_{i1}$  and  $T_{i2}$  from the two besides in-dimer adsorption sites  $A_4$  and  $A_9$  to  $A_i$ .

Figures 9(a) and 10(a) show the location of the adsorption sites for the As ad-dimers and As in-dimer, respectively. The atomic configurations for the adsorbates are given in Figures 9(b) and 10(b), whereas the transitions to/from neighboring adsorption sites are reported in Figures 9(c) and 10(c). Finally Figures 9(d) and 10(d) plot the energy barriers separating these adsorption sites from the neighboring ones.

Tables III and V report the energies for the stable configurations and the corresponding saddle points. Even in this case we have found very high binding energies for these adsorption sites and high energy barriers (around 0.7 eV) that make these configurations very stable once the adatom reaches them overcoming the barriers.

#### IV. DISCUSSION

In order to evaluate the effects of the strain and the role of the different surface reconstructions on the In adsorption properties we now compare our results with the results of similar calculations reported in the literature. To better evaluate the differences we report in Fig. 11 the more common adsorption features as extracted by the literature and the present work. In the same figure we name each specific adsorption site with respect to its position

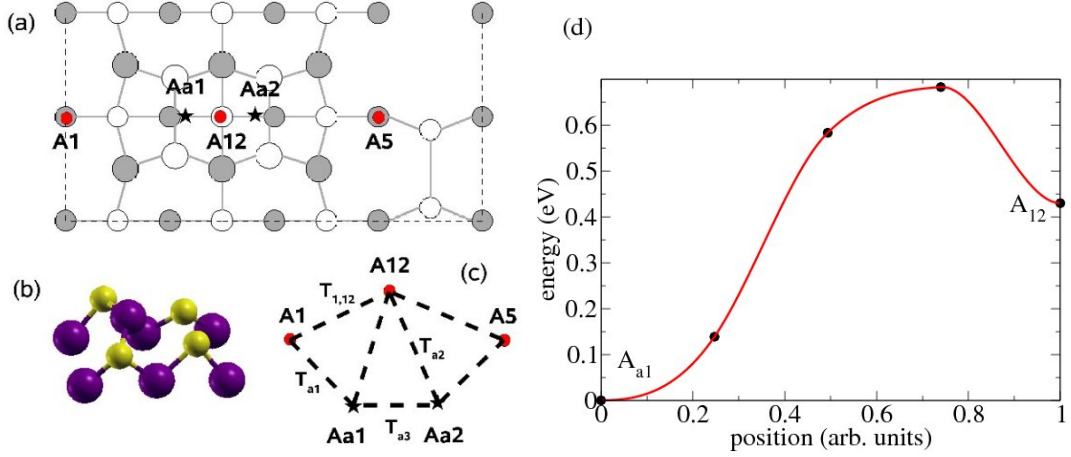


FIG. 9: (Color online) Additional adsorption sites  $A_{a1}$  and  $A_{a1}$  due to the In insertion into the As ad-dimer on the  $\beta_2$  surface reconstruction. (a) The location of the adsorption sites are indicated by stars. (b) Atomic configuration. (c) Scheme of the transitions between the  $A_{a1}$  and  $A_{a1}$  adsorption site and the neighboring sites. (d) Energy profile for barriers  $T_{a2}$  from the top ad-dimer adsorption site  $A_{12}$  to  $A_a$ .

relative to the As in-dimers (i) and ad-dimers (a), and indicate also the reconstructions where these adsorption sites are typical.

### A. $\alpha_2$ vs $\beta_2$ reconstruction (this work)

There are no big differences between the adsorption features on the  $\alpha_2$  and on the  $\beta_2$  surface reconstructions. In particular, the adsorption energy and location differences (see Table IV) between corresponding adsorption sites, are within a few hundreds of meV. The greatest differences are those in the region of the missing ad-dimer where the structural difference between the two surface reconstructions is larger. On the  $\beta_2$  reconstruction the positions and energies of the adsorption sites are modified owing to the symmetry properties of the reconstruction. The most important difference is the presence of the adsorption sites  $A_{3'}$  and  $A_{12}$  on the  $\beta_2$  surface reconstruction, that are absent on the  $\alpha_2$  surface reconstruction. On the contrary, the adsorption sites  $A_{10}$  and  $A_{11}$  of  $\alpha_2$  disappear in  $\beta_2$  transforming into the top ad-dimer site  $A_{12}$ .

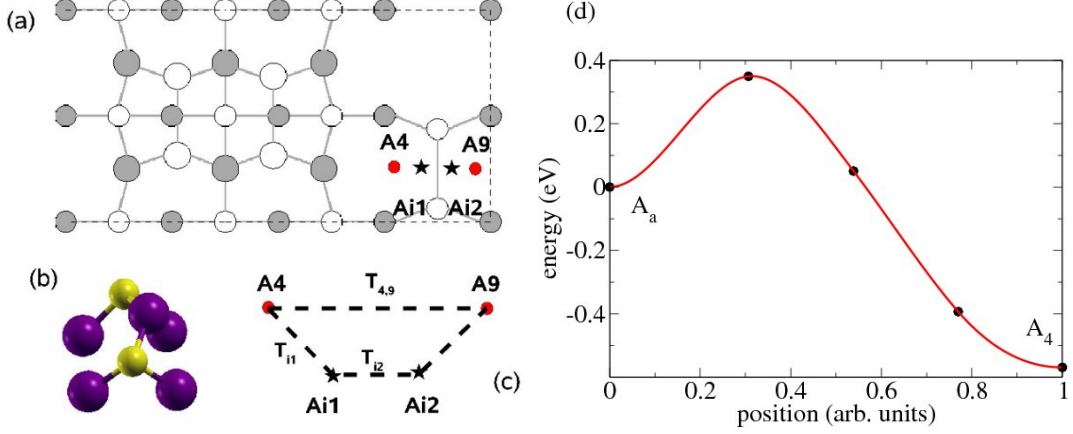


FIG. 10: (Color online) Additional adsorption sites  $A_{i1}$  and  $A_{i2}$  due to In insertion into the As in-dimer on the  $\beta_2$  surface reconstruction. (a) The locations of the adsorption sites are indicated by stars. (b) Atomic configuration. (c) Scheme of the transitions between the  $A_{i1}$  and  $A_{i2}$  adsorption sites and the neighboring sites. (d) Energy profile for barrier  $T_{i1}$  from the besides in-dimer adsorption site  $A_4$  to  $A_{i2}$ .

### B. 1.75 ML InAs on GaAs (001) $\beta_2(2 \times 4)$ vs InAs (001) $\beta_2(2 \times 4)$

In this subsection we compare our results for In adsorption on the  $\beta_2(2 \times 4)$  reconstruction of the InAs WL on GaAs(001) with the results for In adsorption on the  $\beta_2(2 \times 4)$  reconstruction of pure InAs(001) of ref. [21, 22]. The main difference between the two cases is that the InAs WL on GaAs is subjected to a compressive strain on the (001) plane. Thus, the comparison allows us to evaluate the effect of the WL strain on In adsorption. We principally refer to Fig.2 of ref.[21] and to Table VI of the present paper, where we have reported the energies of the minima of In on the InAs surface [33].

In the case of pure InAs[21], only six minima were calculated and their positions on the surface are almost the same as those calculated by us. In particular, only one minimum  $B_8$  in the *bridge in-dimer* position (see Fig. 11) was found halfway between the two equal minima  $A_6$  and  $A_8$  calculated by us for the InAs/GaAs case. The two minima  $A_6$  and  $A_8$  are separated by a relatively high barrier of 300 meV in our calculation. We recall here that for  $\alpha_2$  we calculate barriers only 42 and 142 meV high between the same adsorption sites. ( $A_6$  and  $A_8$  are no more equivalent in  $\alpha_2$ ).

In the case of pure InAs, the *besides in-dimer*  $B_4$  and  $B_9$  show the strongest binding. In

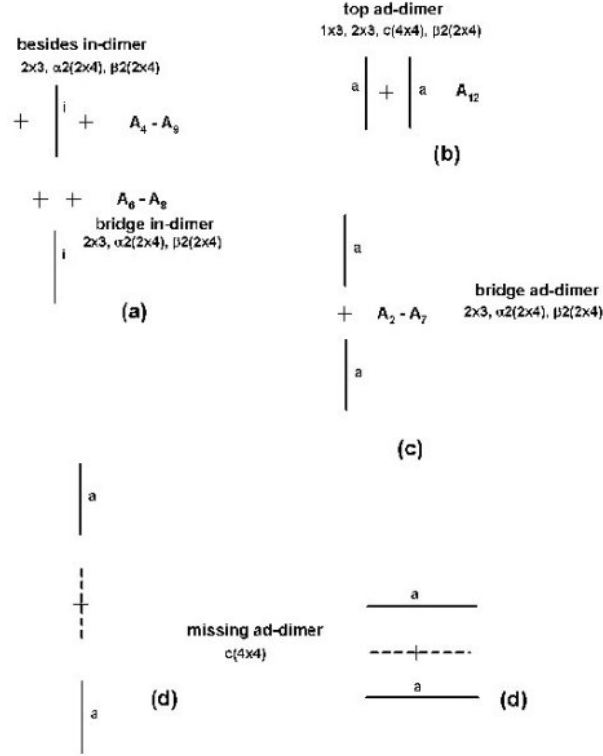


FIG. 11: Scheme of the main adsorption sites for an In adatom on (001) reconstructed III-V surfaces: (a) besides in-dimer and bridge in-dimer locations, (b) top ad-dimer location, (c) bridge ad-dimer location, and (d) missing ad-dimer locations.

the case of the InAs WL on GaAs, instead, the more strongly bonded sites are located at the *bridge in-dimer* positions  $A_6$  and  $A_8$ . From Tables III and VI we see that the energy difference between the sites (4-9) and (6-8) is larger for the InAs WL on GaAs case (240 meV vs 61 meV). It is reasonable to think that this difference is to be ascribed to the strain originated by the lattice mismatch between InAs and GaAs. Also the absence of the shallow adsorption sites corresponding to  $A_1, A_5, A_3$  and  $A_{10}$  could be originated by the absence of the strain.

Nevertheless, it is possible that these differences are originated also by the different grid resolution used for calculating the PES, or by the interpolation algorithms that sometimes are not able to identify correctly the minima or by the difference between GGA used in ref. [21] and LDA used in this work.

### C. In on InAs/GaAs $\beta_2(2 \times 4)$ vs Ga on GaAs $\beta_2(2 \times 4)$

At this stage of the discussion we compare our results for the  $\beta_2$  reconstruction with the results obtained in ref. [20], where the PES of a Ga adatom on the  $\beta_2(2 \times 4)$  surface reconstruction of GaAs(001) was studied. This comparison evidences the different behavior of In and Ga adsorbates, as opposed to the WL composition.

In the case of Ga on GaAs(001) only three minima were reported (without considering the additional minima where Ga breaks the dimers). Two minima are at *bridge ad-dimer* positions while the third one is at a *bridge in-dimer* position. These adsorption sites correspond to the  $A_2$ ,  $A_7$  and  $A_6$ - $A_8$  minima on the InAs WL and to  $B_2$ ,  $B_7$  and  $B_8$  minima of the In on InAs(001) case [21]. These minima are quite stable. Notice the missing of the  $A_{12}$  adsorption site on the *top ad-dimer* location, which is present in the case of the In adsorbate on  $\beta_2$  reconstructed InAs covered surfaces. Also the adsorption sites in the *besides in-dimer* locations are missing in this case.

### D. In adatom on InGaAs surfaces

In this section we compare with the results of ref. [12, 16] where InGaAs reconstructions of the WL on GaAs were considered. The PESs of the In adatom on: (i)  $\text{In}_{2/3}\text{Ga}_{1/3}\text{As}(001)$  ( $2 \times 3$ ) (corresponding to a In coverage  $\theta = 0.66$ ), (ii)  $\text{In}_{2/3}\text{Ga}_{1/3}\text{As}(001)$  ( $1 \times 3$ ) (corresponding to  $\theta = 0.66$ ), and (iii)  $\text{GaAs}(001)$   $c(4 \times 4)$  (corresponding to  $\theta = 0$ ) surface reconstructions were studied. From all these calculations we can see that one adsorption site is always located in a *top ad-dimer* position, in the same configuration of the  $A_{12}$  adsorption site on  $\beta_2$  of this work. The depth of these adsorption sites defined by the height of the lowest barrier confining the adsorbate are: 140 meV, 60 meV, 100 meV, 385 meV and 135 meV for ( $2 \times 3$ ), ( $1 \times 3$ ),  $c(4 \times 4)$ , InAs  $\beta_2(2 \times 4)$  and InAs WL on GaAs  $\beta_2(2 \times 4)$ , respectively. We can see that these minima are not strongly bonded, apart from the case of In on pure InAs(001)  $\beta_2$  reconstructed surface.

The deepest minima are located at the *besides in-dimer* location, both in the case of the ( $2 \times 3$ ) reconstruction of [12] and of the reconstructions studied in this work. In the case of the  $c(4 \times 4)$  reconstruction, stable locations are at the *missing ad-dimer* sites (see fig. 11). In these adsorption sites the In adatom binds to four As atoms below. In the case of

the  $(1 \times 3)$  reconstruction the stable location sees the In atoms bonded to the cations layer below.

## V. CONCLUSIONS

We have carried out a first-principles study of the adsorption properties of an In adatom deposited on a InAs wetting layer on GaAs(001) reconstructed  $\alpha_2(2 \times 4)$  or  $\beta_2(2 \times 4)$ . We have first studied the equilibrium geometry of the surfaces and the relative phase stability with respect to the growth conditions. We have found that, in the case of the InAs WL the interlayer distances are systematically higher than those of pure GaAs, owing to the compressive strain. Moreover, we have found that the  $\alpha_2$  reconstruction of the InAs WL is favored over the  $\beta_2$  reconstruction, for a wider range of growth conditions, when compared to the bare GaAs(001) surface.

We have analyzed the PES for an In adatom determining the adsorption sites and the saddle points for both  $\alpha_2$  and  $\beta_2$  reconstructions. We have found 11 minima in the PES for both reconstructions. Most of them occur in the same positions in both cases. Two minima are instead specific of the  $\alpha_2$  and  $\beta_2$  reconstructions, due to the presence on  $\beta_2$  of an additional As ad-dimer. For the adsorption sites present on both reconstructions, we have studied the change of the adsorption energy and location caused by the presence or absence of the second As ad-dimer. We have identified two low-energy trenches along the  $[\bar{1}10]$  direction, alongside the in-dimer chain, for both  $\alpha_2$  and  $\beta_2$ .

The comparison to analogous studies reported in the literature has revealed some general features for the In adsorption on different surface reconstructions. In particular, we have found that stable adsorption sites are always located: (i) besides the in-dimers, (ii) at the bridge positions between in-dimers, (iii) between ad-dimers (only for  $\beta_2$  which has two adjacent As ad-dimers), and (iv) at the bridge between ad-dimer positions. We have identified also other shallower adsorption sites which are more reconstruction specific and are related to  $\alpha_2$  having a lower symmetry than  $\beta_2$ .

site energy (meV)	
A <sub>1</sub>	220
A <sub>2</sub>	387
A <sub>3</sub>	312
A <sub>4</sub>	49
A <sub>5</sub>	344
A <sub>6</sub>	99
A <sub>7</sub>	559
A <sub>8</sub>	0
A <sub>9</sub>	112
A <sub>10</sub>	868
A <sub>11</sub>	498
A <sub>i</sub>	-100
A <sub>a</sub>	239

TABLE I: Adsorption energies for the In adatom in the different adsorption sites of the  $\alpha_2$  surface reconstruction, relative to the A<sub>8</sub> energy, labeled as A<sub>n</sub>. The labels A<sub>i</sub> and A<sub>a</sub> refer to the configurations of the adsorbate into the in-dimer and the ad-dimer, respectively.

### Acknowledgments

The authors would like to thank A. Ishii for providing us with the data about In adsorption on InAs [21]. We acknowledge the support of the MIUR PRIN-2005, Italy. The calculations were performed at CINECA-Bologna under the grant “Iniziativa Calcolo Parallelo del CNR-INFN”, and at LabCsai in Modena.

### APPENDIX A: ENERGIES OF MINIMA AND SADDLE POINTS

In this appendix we report all the numerical values calculated for minima and saddle point energies.

saddle energy (meV)	
$T_{2,9}$	895
$T_{2,7}$	676
$T_{3,7}$	635
$T_{3,4}$	456
$T_{4,9}$	498
$T_{4,5}$	453
$T_{1,10}$	893
$T_{6,8}$	142
$T_{8,9}$	428
$T_{1,9}$	272
$T_{1,8}$	418
$T_{5,11}$	554
$T_{10,11}$	929
$T_{7,11}$	743
$T_{11,7}$	750
$T_{i1}$	613
$T_{i2}$	493
$T_{a1}$	893
$T_{a2}$	926
$T_{a3}$	1117

TABLE II: Energies of the saddle points in the PES of the  $\alpha_2$  surface reconstruction, relative to the  $A_8$  adsorption energy. The saddle points connecting the minima  $A_n$  and  $A_m$  are labeled by  $T_{n,m}$ , while the labels  $T_{in}$  ( $T_{an}$ ) indicate the saddle points between the minima into the in-dimer (ad-dimer) and the neighboring sites, as shown in Fig. 8 (Fig. 7)

site	energy (meV)
A <sub>1</sub> , A <sub>5</sub>	216
A <sub>2</sub> , A <sub>7</sub>	506
A <sub>3</sub> , A <sub>3'</sub>	323
A <sub>4</sub> , A <sub>9</sub>	240
A <sub>6</sub> , A <sub>8</sub>	0
A <sub>12</sub>	588
A <sub>i</sub>	-330
A <sub>a</sub>	158

TABLE III: Adsorption energies for the In adatom in the different adsorption sites of the  $\beta_2$  surface reconstruction, relative to the A<sub>8</sub> energy, labeled as A<sub>n</sub>. The labels A<sub>i</sub> and A<sub>a</sub> refer to the configuration of the adsorbate into the in-dimer and the ad-dimer, respectively.

site	$\Delta E$ (meV)	$\Delta r/a_0$
A <sub>1</sub>	-134	0.022
A <sub>2</sub>	-7	0.069
A <sub>3</sub>	-121	0.330
A <sub>4</sub>	66	0.168
A <sub>5</sub>	-259	0.350
A <sub>6</sub>	-224	0.100
A <sub>7</sub>	-179	0.588
A <sub>8</sub>	-125	0.018
A <sub>9</sub>	4	0.031

TABLE IV: Adsorption energy differences and position displacements between the In adsorbate for the corresponding adsorption sites of the  $\beta_2$  and the  $\alpha_2$  reconstructions.

saddle energy (meV)	
$T_{4,5}$	392
$T_{5,6}$	424
$T_{1,12}$	976
$T_{12,2}$	723
$T_{2,11}$	727
$T_{2,3'}$	974
$T_{2,7}$	589
$T_{6,3}$	577
$T_{4,3}$	424
$T_{4,9}$	701
$T_{6,8}$	296
$T_{i1}$	589
$T_{i2}$	94
$T_{a1}$	760
$T_{a2}$	610
$T_{a3}$	1024

TABLE V: Energies of the saddle points in the PES of the  $\beta_2$  surface reconstruction, relative to the  $A_8$  ( $\beta_2$ ) adsorption energy. The saddle points connecting the minima  $A_n$  and  $A_m$  are labeled by  $T_{n,m}$ , while the labels  $T_{in}$  ( $T_{an}$ ) refer to the saddle points between the minima into the in-dimer (ad-dimer) and the neighboring sites, as shown in Fig. 10 (Fig. 9).

site	energy (meV)
$B_2, B_7$	302
$B_4, B_9$	0
$B_8$	61
$B_{11}$	163

TABLE VI: Adsorption energies (calculated with respect to  $B_4$  energy) for the In adatom in the different adsorption sites on the InAs  $\beta_2$  surface reconstruction, labeled as  $B_n$  (see ref. [21, 33]). The positions of the minima  $B_n$  corresponds to the minima  $A_n$  in fig. 5(b).

- 
- [1] I. N. Stranski, and L. Karstano, Sitzungsber. Akad. Wiss. Wien, Math Naturwiss. Kl. IIB **146**, 797 (1938).
- [2] C. Ratsch, Phys. Rev. B **63**, 161306(R) (2001)
- [3] P. Kratzer, E. Penev, and M. Scheffler, Appl. Surf. Sci. **216**, 436 (2003)
- [4] E. Penev and P. Kratzer, “First-Principles study of InAs/GaAs(001) heteroepitaxy”, in: *B.A. Joyce et al. (eds.) Quantum Dots: Fundamentals, Applications and Frontiers*, NATO Science Series II, Vol. **190**, p 27-42, (Springer Verlag, Berlin) (2005).
- [5] F. Patella, F. Arciprete, E. Placidi, S. Nufri, M. Fanfoni, A. Sgarlata, D. Schiumarini, and A. Balzarotti Appl. Phys. Lett. **81**, 2270 (2002).
- [6] N. Grandjean, and J. Massies, J. Crystal Growth **134**, 51 (1993)
- [7] P.A. Bone, J.M. Ripalda, G.R. Bell, and T.S. Jones, Surf. Sci. **600**, 973 (2006).
- [8] J.G. Belk, C.F. McConville, J.L. Sudijono, T.S. Jones, and B.A. Joyce, Surf. Sci. **387**, 213 (1997).
- [9] F. Patella, F. Arciprete, M. Fanfoni, and A. Balzarotti, Appl. Phys. Lett. **88**, 161903 (2006)
- [10] P. Kratzer, C. G. Morgan, and M. Scheffler Phys. Rev. B **59**, 15246 (1999)
- [11] E. Penev, “ On the theory of surface diffusion in InAs/GaAs(001) heteroepitaxy”, Ph.D thesis, Technische Universität Berlin (2002)
- [12] E. Penev, S. Stojković, P. Kratzer, and M. Scheffler, Phys. Rev. B **69**, 115335 (2004)
- [13] W. Kohn, and L. J. Sham Phys. Rev **140**, A1133 (1965).
- [14] D. M. Ceperley, and B. J. Alder, Phys. Rev. Lett. **45**, 566 (1980)
- [15] J. P. Perdew, and A. Zunger, Phys. Rev. B **23**, 5048 (1981)
- [16] E. Penev, P. Kratzer, and M. Scheffler, Phys. Rev. B **64**, 085401 (2001)
- [17] W. G. Schmidt, F. Bechstedt, N. Esser, M. Pristovsek, Ch. Schultz, and W. Richter, Phys. Rev. B **57**, 14596 (1998)
- [18] L. Wang, P. Kratzer, and M. Scheffler, Jpn. J. Appl. Phys. **39**, 4298 (2000)
- [19] J. G. LePage, M. Alouani, D. L. Dorsey, J. W. Wilkins, and P. E. Blöchl, Phys. Rev. B **58**, 1499 (1998)
- [20] A. Kley, P. Ruggerone, and M. Scheffler, Phys. Rev. Lett **79**, 5278 (1997)
- [21] K. Fujiwara, A. Ishii, and T. Aisaka, Thin Sol. Films **464-465**, 35 (2004)

- [22] A. Ishii, K. Fujiwara, and T. Aisaka, *Appl. Surf. Sci.* **216**, 578 (2003)
- [23] A. Kley, “Theoretische Untersuchungen zur Adatomdiffusion auf niederindizierten Oberflächen von GaAs”, Ph.D. Thesis, Technische Univ. Berlin (1997).
- [24] C. Stampfl, and C. G. Van de Walle *Phys. Rev. B* **59**, 5521 (1999)
- [25] P. Kratzer, C.G. Morgan, and M. Scheffler, *Prog. Surf. Sci.* **59**, 135 (1998)
- [26] P. Pechukas, *Dynamics of molecular collisions*, Part B (W. H. Miller ed.), Plenum Press, New York (1976).
- [27] D. G. Truhlar, W. L. Hase, and J. T. Hynes, *J. Phys. Chem.* **87**, 2664 (1983).
- [28] D. G. Truhlar, B. C. Garret, and S. J. Klipenstein, *J. Phys. Chem.* **100**, 12771 (1996).
- [29] H. Jónsson, G. Mills, and K. W. Jacobsen, in: B. J. Berne, G. Ciccotti, D. F. Cocker (Eds.) *Classical and quantum dynamics in condensed phase simulations* World scientific (1998)
- [30] G. Mills, and H. Jónsson, *Phys Rev. Lett.* **72**, 1124 (1994)
- [31] pwscf website: <http://www.pwscf.org>
- [32] N. Moll, A. Kley, E. Pehlke, and M. Scheffler, *Phys. Rev. B* **54** 8844 (1996)
- [33] A. Ishii, private communication